SLR Estimation Using CEEMDAN Near the Korean Peninsula

Young Jin Kim
National Institute for Mathematical Sciences
Okyu Kwon
National Institute for Mathematical Sciences
Hark-Soo Song
National Institute for Mathematical Sciences
Jongho Kim
National Institute for Mathematical Sciences
Hyuk Kang (kh9395@nims.re.kr)
National Institute for Mathematical Sciences

Research Article

Keywords: SLR estimation, CEEMDAN, Korean Peninsula, sea levels, global warming, international scope, Intergovernmental Panel on Climate Change (IPCC), El Niño-Southern Oscillation (ENSO)

Posted Date: November 1st, 2021

DOI: https://doi.org/10.21203/rs.3.rs-1011105/v1

SLR estimation using CEEMDAN near the Korean Peninsula

Young Jin Kim[1,*], Okyu Kwon[2], Hark-Soo Song[1], Jongho Kim[1], and Hyuk Kang[1,+]

[1]Public Data Analysis Team, National Institute for Mathematical Sciences, Daejeon 34037, Korea
[2]Research team for transmission dynamics of infectious disease, National Institute for Mathematical Sciences, Daejeon 34037, Korea
[*]kimyoungjin06@nims.re.kr
[+]corresponding author

ABSTRACT

The rise of sea levels due to global warming is a problem of concern at an international scope and the causes are already known relatively clearly. Every year, the Intergovernmental Panel on Climate Change (IPCC) creates a scenario for greenhouse gas emissions and predicts the global average sea-level rise rate accordingly. It is necessary to estimate the rate of sea-level rise to date in creating such a scenario. In particular, since the height of the sea level changes (SLC) continuously, the errors of SLC may occur due to various causes with a fragmental analysis. To estimate the sea-level rise accurately, we applied Complete Ensemble Empirical Mode Decomposition with Adaptive Noise (CEEMDAN) is based on the Empirical Mode Decomposition (EMD) to decompose the tidal level. Through this, we discover that the differences in the local sea-level rise rate occurred even within a small area. To understand each component of tide level decomposed through CEEMDAN, we confirm the component-wise/regional correlation between tidal stations. In addition, we looked at how local sea-level rise correlated with the global meteorological phenomenon, El Niño-Southern Oscillation (ENSO) which is one of the most influential recurring climate patterns Socioeconomically.

Introduction

Global warming, which began in earnest in the late 19th century, continues to accelerate until now. It is a hot issue in the world that global warming and its resulting environmental change. The Sea level rise (SLR) is one of the representative results of global warming, and it is analyzed through various interdisciplinary approaches. How will global warming affect SLR? The first thing you can think about the polar glaciers. The melting of polar glaciers and the resulting seawater flows into the sea, causing a direct rise in sea level[1]. In addition to this, there may be various causes of SLR, and research related to this is ongoing[2–7]. Church *et al.* compared the effects of various causing - thermal expansion, ice sheets, glaciers, and groundwater - and showed that the sum was consistent with the observed rate of SLR on a global scale[2]. DeConto and Pollard predicted Antarctica's contribution to Global Mean Sea Level (GMSL) by simulation with two dynamics coupling - ice sheet dynamics and climate dynamics[3]. Rignot *et al.* confirmed the loss of 252 billion tons of sea ice per year on the Antarctic Thwaites Ice Sheet, four times more than 40 years ago[4]. B. Horton *et al.* reported that the ice sheets in Greenland and Antarctica were the most impactable cause of the uncertainties related to climate change and SLR[5]. According to Horton *et al.*, SLR in the 20th century occurred as glaciers melted. But in the past 20 years, it was caused by the melting of the Greenland and Antarctic ice sheets mostly. From 1992 to 2017, the ice melting is six times faster, and only 6.4 trillion tons of ice disappeared. In addition, the ice sheets in Greenland and West Antarctica are equivalent to global 13m SLRs, and it shows that when the relatively stable South Antarctic ice sheet melts, the sea level can rise to 50m.

There are studies using satellite data. They determined the mass change of the ice sheet and the resulting global average SLR by tracking the change in ice sheet height using satellite data[6,7]. Smith *et al.* found that Greenland's shrinking ice sheet and ice loss in Antarctica were responsible for an SLR of 14 mm since 2003. It is a little less than a third of the total sea-level rise observed in the world's oceans[7].

There are several applied studies about effects on the overall natural and social society environment caused by SLR. Robinson find migration patterns in USA[8]. Many studies consider linking SLR and coastal flooding[9–15]. According to these studies, SLR and the increasing trend of coastal flooding phenomena have a significant correlation.

As with the results of the above studies, the causes of SLR are generally sufficiently studied with quantitative interpretation, and related studies are still ongoing. However, most of the previous studies refer to the average rate of SLR on a global scale. On the other hand, the rate of SLR is not uniform worldwide and can vary regionally. As the thickness of the ice sheet at the

eastern part of Antarctica has become thicker in recent years[7,16], the average sea level is rising more and more from a global point of view, but the rate of increase varies regionally. At the local scale, there are places where the change in sea level is significantly different within a small area, or there are areas where the sea level is lowering regionally, as in the vicinity of the Baltic Sea in Northern Europe.

Is there any reason to look into the Korean Peninsula? The most extreme tidal current in the world is the Saltstraumen Strait in Norway, the strongest with a maximum speed of 41 km/h, in the vicinity of the Gulf of Fundy, which locates on the border between Canada and the United States, the ridge reaches 17 m. Despite the relatively narrow topography of the peninsula, the Korean peninsula shows various tidal phenomena characteristics. On the west coast of the Korean peninsula, the maximum tidal difference even reaches 9m. On the other hand, at least 0.2m is seen on the East coast, which is about 300km away from the west coast in a straight line. The southern coast, the tip of the Korean peninsula, is an archipelago area with many small islands and complex sea currents. In addition, tide data over a maximum of 50 years are accumulated on the Korean Peninsula, and enough tide measurement stations are placed and operated in a small area, so it has many advantages in examining the tide level. In addition to the topographical characteristics, it is located in the mid-latitude climate and has a temperate climate with distinct four seasons affected by various air masses around it, but the recent global warming has changed it to a subtropical climate. Oceanographically, the east coast is connected to the Pacific Ocean in the distance and belongs to several environmentally special regions where the cold and warm currents meet to form the boundary of water masses.

One can measure the rate of SLR in a variety of ways. There is two kind of data - Satellite data and tidal data - to estimate the rate of SLR relatively directly, and each has different advantages and disadvantages. Satellite data, which are mainly used to estimate the rate of SLR on a global scale, have measured the global sea surface height at approximately 10-day intervals with accuracy better than 5cm since 1992 by TOPEX/Poseidon, and the following satellites have better accuracy and resolution[17]. In addition, since satellite data uniformly measures the amount of change in sea level height with relatively good resolution (about 10 km unit grid) for the whole of the world, it is possible to measure the rate of SLR uniformly at the global scale. The rate of SLR in the ocean can be measured relatively accurately, but the sea level near the shoreline is inaccurate due to the limitation of the measurement method[18]. Hamlington improved the accuracy by combining with tide gauge to estimate the rate of SLR near the shoreline[18]. Although such advantages of satellite data, tidal data still have many strengths to evaluate the local SLR rate near the shoreline. The tidal data are distributed sparsely in a local area in contrast with satellite data. Contrastively, the tidal data is accumulated over a long period, and a European tidal station has been operated for more than 200 years. However, as the history is long, it is possible to change the method or equipment of measurement, so quality (or resolution) can not be uniform. It can be disadvantaged to the inhomogeneity of the measurement qualities between stations. Finally, most measurement stations provide tidal data at 1-hour intervals after measuring at intervals of a few seconds to minutes, and then data purification, so it can be easy to analyze a more detailed time series of tide levels. As above properties of both data, it is better to choose data according to the purpose.

Many studies have performed an estimation of SLR rates using satellite data[19–25]. These studies generally focus on a global trend with all data on the surface of the planet. On the other hand, the SLR estimation with tidal data has a limitation to a region of interest. Because almost tidal stations can be located only on the coast, although the tide is over the entire earth, and accurately estimate the optimal SLR rate in a more local region[23,26–29]. In addition, in most studies, linear regression or quadratic regression analysis is applied to estimate the SLR rate after a correction like considering Vertical Land Motion (VLM) on the Global Positioning System (GPS). However, some studies estimated SLR rates using new methodologies[20,23–25]. The above studies use an applied methodology like EMD[23] or Empirical Orthogonal Function (EOF)[20,24,25]. Kim used Ensemble Empirical Mode Decomposition (EEMD) and CycloStationay Empirical Orthogonal Function (CSEOF) to estimate the rate of SLR with tidal data[23,24]. Cabanes and Nerem applied EOF and CSEOF to satellite data to estimate the rate of SLR[20,25]. It is an attempt to take one step in the existing research by applying the brand-new algorithm.

In this study, we investigated the longer-term trend of SLR and differences in local SLR rates. We estimated the local SLR rate nearby the Korean peninsula using tidal data measured up to 50 years. Especially, not using conventional methods, we estimate the SLR rate more elaborately with a new methodology - CEEMDAN is more advanced than the previous EEMD study[23]. The SLR rate is compared with obtained using linear regression and EEMD to examine the differences. In addition, indirectly, to prove the validity of decomposed mode using CEEMDAN, we investigate the periodicity of the IMF at the same level using Fast Fourier Transform (FFT). In addition, we confirmed the correlation with ENSO indices, which is one of the representative global climate indices.

Results

SLR estimation

The fact that the regional SLR rate is different is taken for granted, just like the regional temperature rise due to global warming can be different. However, it is not easy to analyze and understand the causes or mechanisms because the climate system is too complex. Therefore, we tried to understand the phenomenon of SLR rather than analyzing the cause itself. To estimate the

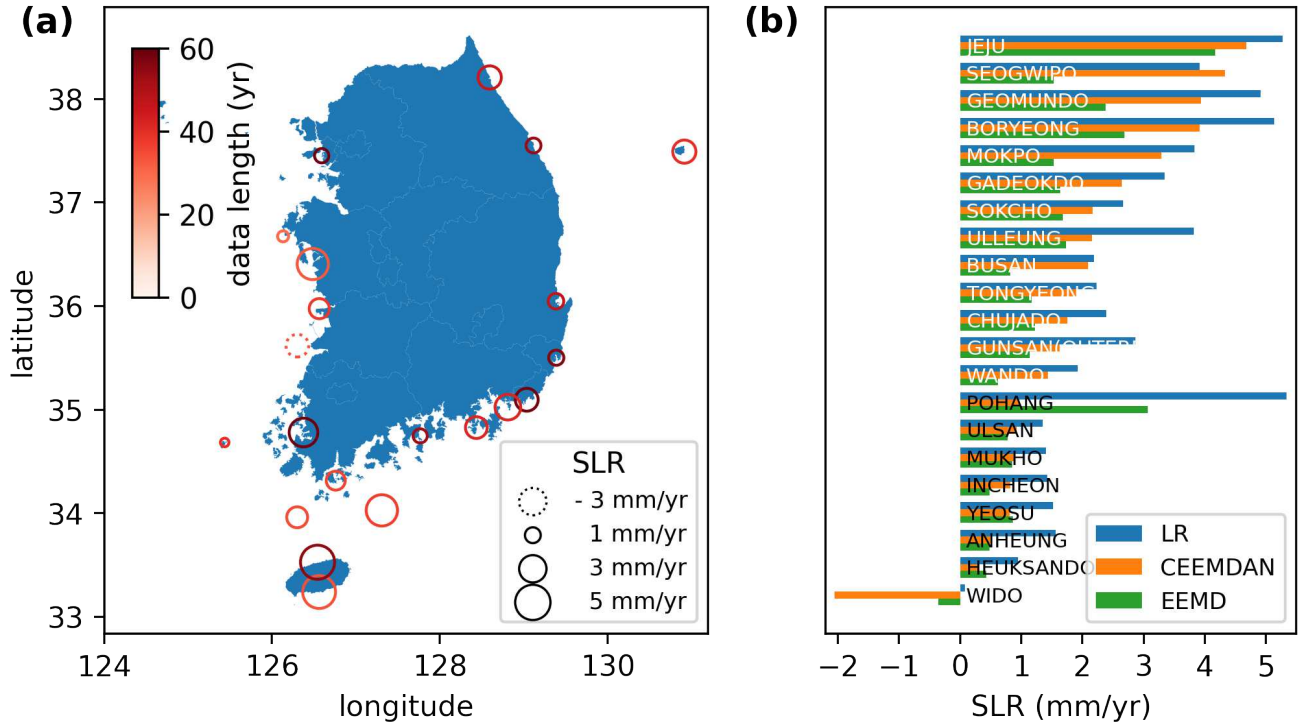

Figure 1. Sea Level Rise (SLR) estimation nearby the Korean Peninsula. (**a**) The SLRs map using CEEMDAN and (**b**) a comparison of three SLRs with Linear Regression(Blue) and CEEMDAN(Orange), and EEMD(Green). All 21 tidal stations have cumulated data for more than 20 years. The local difference of SLR is observed. The CEEMDAN usually estimates SLR similar to LR except for Pohang and Wido.

rate of SLR, we used a total of three methods for comparison - linear regression, EEMD, and CEEMDAN. Considering the last component of results of CEEMDAN as the longest trend with removing a periodic component, the mean SLR rate was obtained from this last mode. The result is shown in fig.1. Overall, all three methodologies showed a similar trend in the rate of SLR among measurement stations. However, there is a tendency in many stations that linear regression measured higher and EEMD measured the lower. In the cases of Pohang and Wido, the difference of SLR between methodologies was bigger. In the case of Pohang, the highest SLR rate measurement in linear regression was 5mm/yr, whereas in CEEMDAN it was only about 1mm/yr. In the case of the Wido station, two EMD-based methodologies - EEMD and CEEMDAN - estimate the sea level decreased. In Supplementary Information S1, it discusses the detailed reasons and related issues. Looking at the results of the SLR rate, the overall trend of the east, west, and south coasts was not similar, but the rate of SLR at each tide station was independent. The cluster showing a similar rate of SLR was the southernmost cluster on the Korean Peninsula near Jeju, Seogwipo, and Geomundo, and this region has the highest SLR rate near the Korean Peninsula. It is confirmed similarly in the results of all three methodologies. Figure 2 shows the SLR rates obtained by CEEMDAN at each station. Figure 2 (**a**) shows the cumulative-SLR from the start of the data, and (**b**) shows derivative-SLR. There is a difference between mean-SLR (Fig. 1), cumulative-SLR (Fig. 2 (**a**)), and derivative-SLR (Fig. 2 (**b**)). In the cases of Boryeong and Geomundo, where mean-SLR is similar (Fig. 1), if you look at the cumulative-SLR and derivative-SLR in Fig. 2, it appears that the sea level in Boryeong did not rise but slightly fell in the last years. In addition to Boryeong, there are some stations with decreasing of sea level in the latest years. In the case of Mukho, the sea level decreased until about 1980 and started to rise at that time. And the cumulative-SLR changed to positive around the late 2000s. SLR rate estimation using EMD has a limitation in that the rate of SLR is converged to zero at both boundaries of the interval because the methodology uses local extremes. To confirm the boundary-dependency of the CEEMDAN, we test the same method (CEEMDAN) at the overlapped sub-sections in the Supplementary Information S2. As a result, it was confirmed that there is a numerical difference between the results at the same overlapped subsection, but the SLR tendency itself does not change significantly, and it is confirmed that the longer the section is more stable.

Figure 3 (**a**) shows the annual average tide level, the last mode of CEEMDAN (long-term trend), and the fitting line of linear regression at the Jeju tidal station. In the case of Jeju, as can be seen from Fig. 2, the SLR rate (CEEMDAN) did not appear to have risen uniformly. It rose sharply around 1970 - 1980 and 1990 - 2000, and recently showed a slowing trend. The

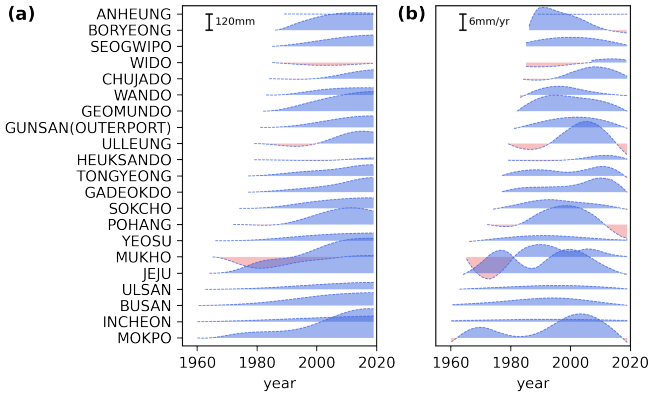

Figure 2. Sea Level Rise(SLR) comparison between tidal stations. (**a**) Cumulative sea-level change(SLC) and (**b**) its derivative: SLR. The first advantage of the estimated SLR using CEEMDAN is that obtained SLR is temporal. The SLC is not monotonous increasing, and it is nonlinear. Two tidal stations(Ulleung and Pohang) are decreasing in 2020.

SLR (CEEMDAN) well reflects the trend of the annual average tide level than the linear regression. Figure 3 (**b**) shows yearly fluctuation and seasonal variability. The yearly sea level is the highest in August when the water temperature is the highest. The seasonal variability differed by about 500mm in Jeju from the lowest February to the highest August. The seasonal variability does not change significantly in the past and present.

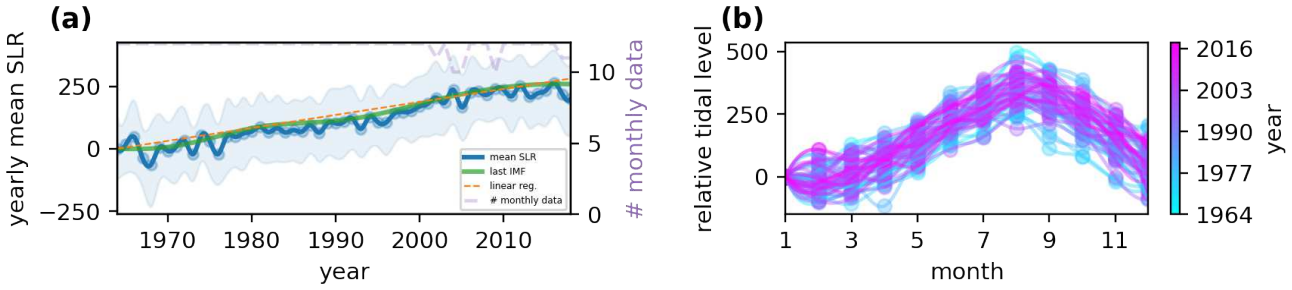

Figure 3. Yearly Sea Level Change(SLC) and seasonal variability in Jeju tidal station. (**a**) annual average SLC(blue), estimated SLR using CEEMDAN(green), and Linear Regression(orange dotted). A dotted purple means the number of monthly data (yearly data content). (**b**) shows yearly fluctuation from 1964 to 2018. In a year, the monthly tidal level is highest in August and lowest in February. The Korean Peninsula, including Jeju, belongs to the Northern Hemisphere and has four seasons distinctly.

Correlation between Stations

We decomposed a tidal level into modes for each frequency (period) by using CEEMDAN. As a result, it was possible to observe that the SLR was not globally correlated, but differed locally at each station on the coast near the Korean Peninsula. So, we measure similarity between tidal stations using equivalent mode. Figure 4 show correlations map between equivalent signal — original-original, first IMF-first IMF, and last IMF-last IMF. The correlation may appear differently depending on the original signal and each mode. The original signal consists of monthly average tide data. Therefore, it is impossible to consider movements and deviations more detailed than the month level. The most prominent movement in monthly tides is seasonal movement. Because the Korean Peninsula is located in mid-latitude, the four seasons are distinct. And the tide level is highest in August in summer, and lowest in February in winter, due to thermal expansion. Therefore, when measuring the correlation with original monthly data, many stations have a very high correlation due to seasonal movement. For the first mode, it is the correlation with the shortest period. So it shows the correlation of tiny deviation like noise. Usually using EMD, the 1st and 2nd IMF are considered as noise and don't use in the analysis in any case. But, it can depend on the characteristics of the data and the purpose of the study. In the case of our data, since it is the monthly average tide, it is reasonable to think there are no noise-related motions. So the correlation for the first mode is meaningful enough. Figure 4 (**b**) show locally correlated stations in the Korean Peninsula. In particular, it was confirmed there are high correlations between the stations on the southern coast of the Korean Peninsula. There is no direct evidence about the reference of local correlation like ocean currents. So, quantitative

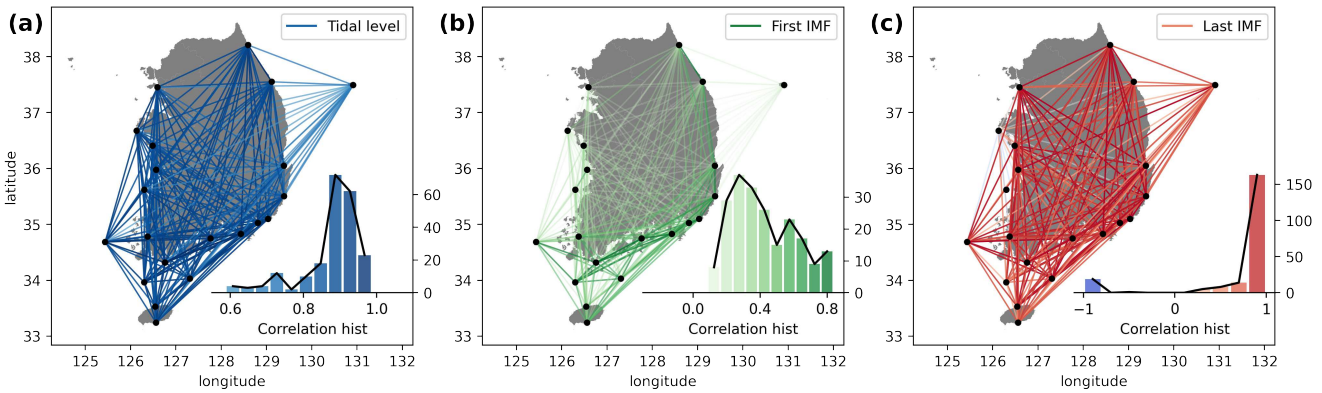

Figure 4. Correlations between tidal stations. The correlations are obtained with (**a**) the original monthly tidal level, (**b**) the first IMF, and (**c**) the last IMF. The correlation is calculated using Pearson correlation. (**a**) The original data is highly correlated with each other by seasonal fluctuation. (**b**) The first IMF is a mode with the most high-frequency signal from the monthly tidal level. (**c**) The last IMFs are also highly correlated with each other because of the monotonic increase, and it does not show any meaningful result. There is an obvious geographical correlation between close stations in the south sea area.

comparisons are impossible without any related data. Nevertheless, the correlation with the first IMF seems to be correlated with ocean currents near the Korean Peninsula by some secondhand reference[30]. Various currents pass on the coast of the Korean Peninsula. In particular, the Kuroshio Current moving northward from the North Equatorial Current affects the entire southern coast of the Korean Peninsula. It was confirmed that the southern coast of the Korean Peninsula was affected by the Kuroshio Current, and the northern tip of the east coast was affected by the North Korean Cold Current - a tributary of the Liman Current. These areas showed a relatively high correlation in a short time scale (months). Also, the correlation on a relatively long-term scale (decade years) is shown in Fig.4 (**c**), but it is difficult to find any meaningful results. The reason can be seen in Fig.2. The Cumulative Sea Level Change (CSLC) is almost ascending at every moment in most of the stations. Therefore, the correlation between the ascending form of CSLC is inevitably measured close to 1. For this reason, in Supplementary Information S3, the correlation was measured using the derivative SLC (Fig.2 (**b**)). In (**a**) and (**b**) of Fig. S3, local similarity could be observed as in (**a**) and (**b**) of Fig.4. For the last IMF(Figure. S3 (**c**)), there were some highly correlated stations in Fig. S3 (**c**). But it is hard to find a meaningful interpretation point for their correlation pattern related to local similarity, specific waters, or specific currents.

Mode dependency

Is it meaningful to look at all the correlations of IMFs with equivalent-level? A mode cannot be correlated with others from the same data since each is a decomposed component. Otherwise, if two equivalent-level modes from different stations have a similar period or frequency, the two modes can be significantly correlated. Or one can ask these questions as 'Each mode decomposed through CEEMDAN represents a specific period, and what does it mean?' or 'Do modes with equivalent order have similar periodic features?'. Unfortunately, because the EMD-based methodology is dependent on the data entirely, it is essential to check whether each mode has a similar periodic feature quantitatively. As a result, it isn't easy to find and compare the periods representing each mode. Because the length of the data measured at each measurement station isn't the same and since the EMD methodology itself is a data-driven method, the number of modes may vary. Even if the total number of modes is the same, each mode doesn't represent the same periodic feature. We attempt to find the frequencies representing each mode through FFT and compared them (Fig. 5). As a result, as mentioned above, the frequency representing each mode doesn't exist. And it is still impossible to completely separate each mode from the original data, so it seems that the mode mixing problem remains.

Correlation with ENSO Indices

We look into the long-range correlation. However, rather than a simple long-range correlation, we would like to examine the correlation with ENSO indices. The ENSO index is an indicator that can represent global phenomena. ENSO indices can indirectly predict El Niño events. The El Niño is a representative abnormal climate phenomenon observed from a very long time ago. Relatively recently, it is revealed that the El Niño phenomenon is not a simple regional meteorological phenomenon but a global quasi-periodic climate phenomenon[31–36]. The El Niño and La Niña events are collectively called the Southern Oscillation or ENSO. The ENSO occurs when the tropical eastern trade winds weaken and has a cycle of about 3 to 7 years. The ENSO is interesting because it has been shown for the first time that it is not just local weather events and is a part of global climate phenomena[32–34]. Recently, due to global warming, this abnormal climate phenomenon has become more frequent, and

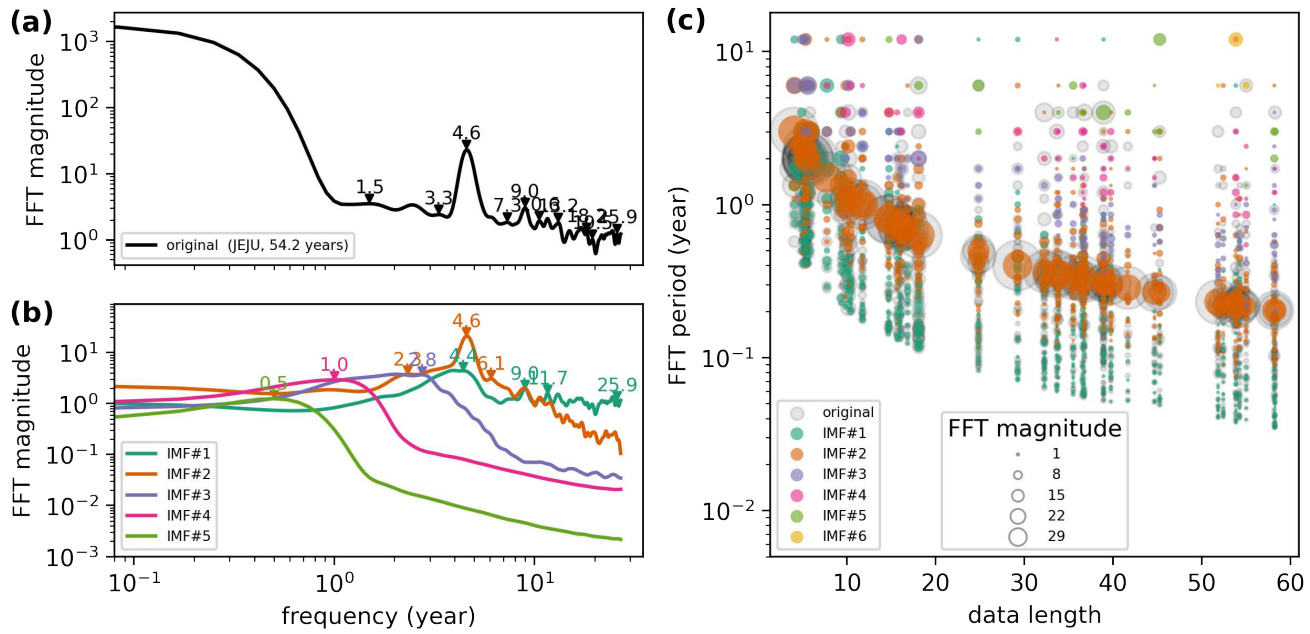

Figure 5. The frequency distribution analysis of each IMF in tidal level by Fast Fourier Transform (FFT). (**a**, **b**) show the FFT result of Jeju station using (**a**) the original tidal level and (**b**) IMFs of tidal level. Although the original tidal level has a specific period (4.6years), each IMF has an undisclosed period in the original tidal level. (**c**) shows the period of modes of CEEMDAN in all tidal stations. They have a specific period in the same IMF. But the result of CEEMDAN is dependent on the data length, so every same IMF in all stations cannot be matched to a typical period.

many research results say that the changed environment has a significant impact not only on fisheries but also on agriculture, commerce, economy, and society[31]. In December 2015, the most prodigious super El Niño occurred in recorded history. Cherry blossoms bloomed in Washington DC, and the winter season temperature rose to 24°C in Japan. The southern coast of the Korean Peninsula also experienced unusual weather events, such as rise water temperatures, cold waves arriving late, and rain instead of snow. However, the El Niño occurs irregularly with its increase/decrease feedback, and related studies are still being actively conducted[35]. In particular, there have also been attempts to predict abnormal climate events through ENSO[36].

We examined the correlation between SLC and ENSO in each region of the Korean Peninsula. The tide data of each tidal station has a monthly average value, and each mode was decomposed via each frequency using CEEMDAN. ENSO indices also have a monthly average value, and there are three representative ENSO indices - Southern Oscillation Index (SOI), Oceanic Niño Index (ONI), and Multivariate ENSO Index (MEI) -depending on the measurement method. After mode decomposition of each ENSO index using CEEMDAN, the correlation between modes was calculated with a time lag for the geographical distance difference. As a result, the correlations are approximately 0.1 to 0.3 and also show a local difference. In particular, some tidal stations(Gunsan, Wando, and Anheung) located in the central part of the West Sea have a relatively high correlation near 0.3 with the SOI. On the other hand, in the case of the Incheon tidal station at the northernmost part of the West Sea, the correlation is only about 0.1. Although slightly different from the local correlation with SLR, the tidal stations in the central of the West Sea and south coast have similar values. There is still insufficient evidence to judge that the regional correlation is obvious. Also, the correlation with ONI or MEI is smaller than that of SOI (Figure 6). And the regional distributions of correlation for each tidal station and each ENSO index have a difference (Supplementary Information S4). So, the interpretation should be careful. This correlation for ENSO and SLC is a correlation between two regions that are about 10,000 km apart. Generally, a value of 0.3 is difficult to say that they are correlated. However, considering the distance between the two regions and also the heterogeneity of data between temperature and SLC, if the value of 0.3 is a significant number, we can't indiscreetly determine that the two phenomena are not correlated completely. The meaning of correlation has to think more deeply.

Discussion

We first estimated the rate of SLR by using tide data of each tidal station in the Korean Peninsula. Although the vicinity of the Korean Peninsula is a small area with latitude 5° and longitude 5°, rates of SLR are very different within this small region. The tidal level has a local difference, and it looks like to fluctuates as a mixing state in various periods such as daily, monthly, and

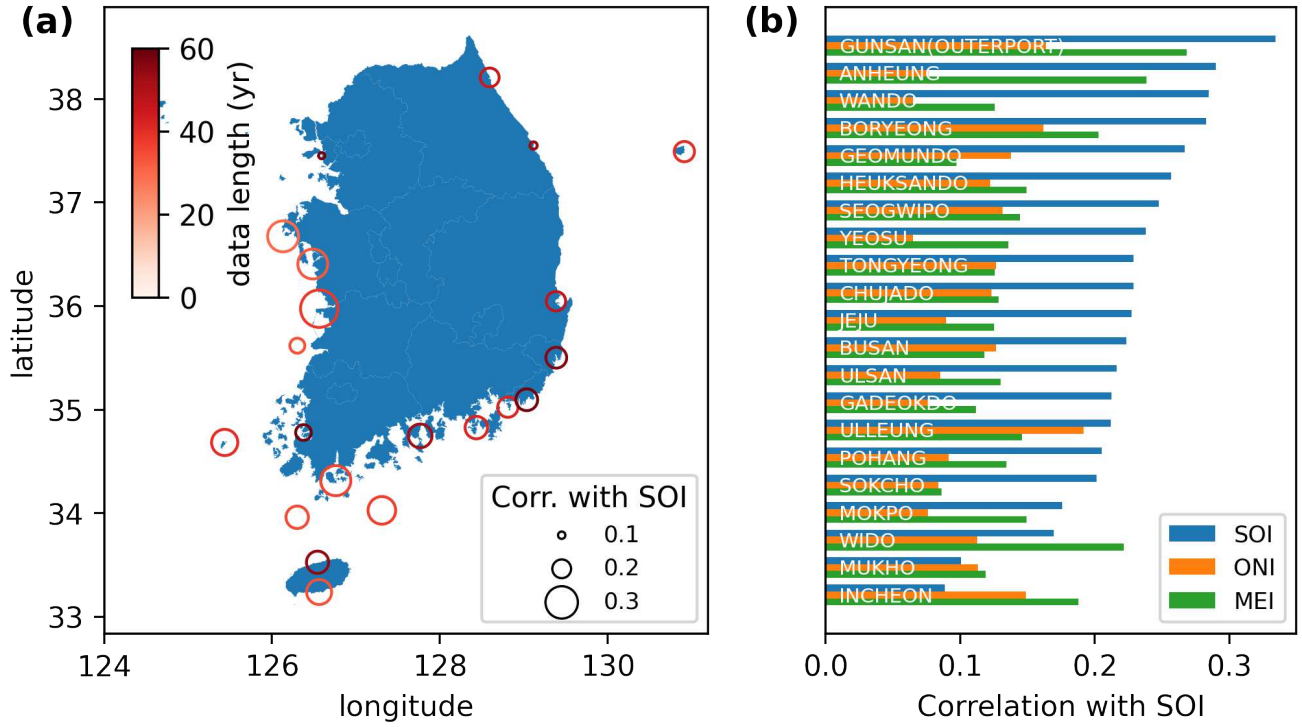

Figure 6. Correlation with ENSO indices. (**a**) a correlation map with Southern Oscillation Index (SOI) and (**b**) a correlation of each station with three ENSO indices. The Middlewestern area has a higher correlation with SOI. Sea level changes correlated poorly with ENSO indices, but they are not tiny to be ignored. The correlations with three ENSO indices don't have a common tendency.

yearly periods. To extract these periodic components, the EMD is applied to the tidal level with CEEMDAN. As a result, local differences in tide data on the Korean Peninsula were revealed. Previously, according to Smith *et al.*[7], the global SLR rate has increased by approximately 45mm since 2003. However, the average rate of SLR in the Korean Peninsula is higher than that. In addition, there is also a place where is no local increase at all and rather decreases as average during two decades. Although SLR is a global phenomenon, it can be observed that not only does the rising rate differ locally in a narrow area like off the coast of the Korean Peninsula, but there are also places where the deviation is so significant.

We decompose the monthly average tide data by period using CEEMDAN and estimate temporal SLR using the last mode removing all periodic components as a long-term movement of the sea level. However, anyone can easily recall the question of whether it is appropriate to analyze tide data through an EMD-based methodology. Quantitative estimation of the SLR rate is one of the popular subjects. But the method isn't developed and still is uniform to estimate quantitatively. When analyzing tide data and satellite data, most of them perform regression analysis using the most basic linear regression or quadratic terms. Most of these studies consider only well-known seasonal cycles. And the result shows only the mean value of the SLR rate. Estimating the rate of SLR through CEEMDAN not only has the advantage of view a variety of periodic components separately but also can obtain time-series of SLR rate removing the periodic component. Although we cannot answer how the estimation of the rate of SLR is accurate, to check in a roundabout way, we compare it with the result of linear regression analysis, and both results have a similar trend. And this is a new attempt to understand the SLR, and there is sufficient possibility to obtain a new interpretation if a more in-depth study is involving.

To know which periodic component each mode represents, careful interpretation is required because the total length of data measured at each station is different. We confirm CEEMDAN itself has a dependency on data. But we cannot find a meaningful pattern between the periodicity according and the order of each mode. In addition, the result of decomposition may be affected by other factors as the relative size of the tidal difference. Therefore, it is not reasonable to compare the modes for each tidal level as itself, and it is necessary to compare proper modes with each other after examining the periodicity of each mode. Of course, the algorithm itself may have limitations. You can find the mode mixing between first mode (IMF#1) and second mode (IMF#2) in Fig. 7. Not only the development of the methodology itself but also the interpretation of the results should be developed through more research in the future.

This study started with a question about local differences in the rate of SLR. In the long-term trend, local differences in the rate of SLR are evident, and the rate of SLR could be quite different even in the immediate vicinity. However, in the short-term trend, the region sharing the same sea current can be highly correlated due to the influence of the sea current. In this work, we only consider the tidal level to examine the correlation, and the results are only qualitatively related to the flow of ocean currents. One can consider the tidal levels together with sea current in the future to see a confident relationship between the two different data.

Methods

Regression

We performed a regression analysis, one of the most traditional analysis techniques to understand the pattern of data, using the time series of tide data to obtain the SLR rate. Regression analysis refers to a method to fit original data with the target function and get its parameters: the rate of SLR in this case.

We perform Linear and Polynomial regression of order 2 with acceleration term. If the data were sufficient (more than decades), the two results did not differ significantly in the SLR rate for the fitting interval, but the future SLR rate can be different. In the Eq. 1, it is a linear fit with $a = 0$, and vice versa is second-order polynomial regression with acceleration. The regression is optimized to minimize the Root Mean Square Error (RMSE).

$$f_{polynomial\,fit} = ax^2 + bx + c \tag{1}$$

Complete Ensemble Empirical mode decomposition with Adaptive Noise

EMD[37] is a method that decomposes the original signal, which is a mixture of various sine-wave-like sub-signals, into individual modes with its unique frequency. Unlike Fourier Transform (FT), which is often compared with EMD for similar propose, expresses the original signal as the sum of infinitely many sine functions, EMD does not require a basis function. EMD is developed to analyze nonlinear and nonstationary signals. It is difficult to apply FT to nonlinear and nonstationary signals. But EMD can be applied to nonlinear signals and can decompose using only the local extrema without specific a basis function. Each mode obtained from the EMD is called an IMF, and the original signal x can be re-obtained by adding all the decomposed IMFs again. As mentioned above, since these IMFs are obtained without an objective function, they represent a complete data-driven waveform without a specific mathematical form.

EEMD[38] is a method to overcome some of the shortcomings of EMD. EMD causes a mode-mixing problem. It means some separate modes which should be decomposed into different IMFs are mixed due to noise included in the original signal. In EEMD, to solve this problem, the ensemble is used. If white noise is added to the original signal, the effect of inherent white noise is eliminated through the ensembling of multiple EMD analyses. Although EEMD had sufficient advantages over EMD just by using an ensemble, it was discovered decomposition with simple adding noise may not be complete. Mode mixing in which the number of IMFs varies has emerged as a new problem.

CEEMD (Complementary EEMD)[39] uses specific pair of ensembles with effective noise adding to solve the problems. In a pair of ensembles, EMD is performed by adding the same white noise to one side and subtracting it from the other side. Although EEMD guarantees the completeness of the decomposition with a higher probability, there is still a critical problem no guarantee the same number of IMFs.

CEEMDAN[40,41] effectively solved the previously unresolved problems. The existing methodologies calculate each IMF parallelly and average at the end. In contrast, CEEMDAN shares IMF in all ensembles, and all residues are equivalent in the same decompose step. After obtaining each first IMF in each EMD, CEEMDAN gets the average IMF immediately. It is equal to EEMD but the following process is different to get a second IMF. All the ensembles use the common residual removed from the original signal to solve the problem that the number of modes is different. Also, in the early CEEMDAN, an independent white noise is added to the common residual when each IMF is calculated[40]. However, in the improved CEEMDAN, EMD is separately performed on the white noise $n(t)$ added at the beginning of the ensemble, and analysis is performed by adding the residuals of the white noise matching the residuals obtained by removing the average IMF from the original signal at each stage.[41].

SLR estimation

In this study, EEMD and LR were used to compare with the analysis results of CEEMDAN. First, in LR, The value of b in eq. 1 was used as the estimated SLR rate. In CEEMDAN, if an appropriate number of ensembles is used, the last mode becomes the long-term trend without the periodicity of tide data. Therefore, the rate of SLR can be equivalent to the shift of the last mode which all periodic components are removed. However, the case of EEMD is different. In the case of EEMD, if the same number of ensembles in CEEMDAN is used, EEMD gets an additional mode. It is judged as the same term as acceleration equal to a in

eq. 1. Therefore, when estimating the rate of SLR through the EEMD, the second last mode was considered as a long-term trend to understand the SLR and estimate the rate of SLR. For more detailed method is in Supplementary Information S5.

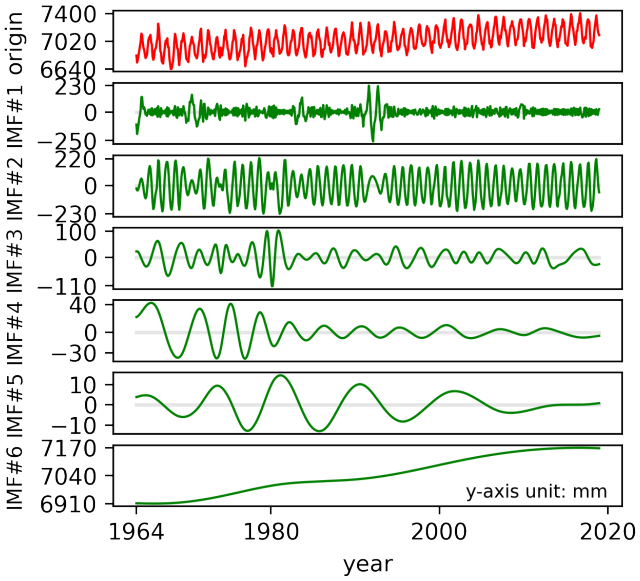

Figure 7. A result of CEEMDAN of Jeju tidal station. The CEEMDAN decomposes the original tidal level of Jeju to each Intrinsic Mode Function (IMF). The original signal shows seasonal fluctuation. The sum of all IMFs equals the original tide level. The last mode (IMF#6) is a monotonic residual decomposed into all oscillation components. Although the CEEMDAN is one of the latest algorithms of EMD, there are still mode mixing problems. In this Jeju case, IMF#1, IMF#2, and IMF#3 are mixed near 1970, 1980, and 1990.

Data

Ocean data is managed by the Intergovernmental Oceanographic Commission (IOC) through the Global Sea Level Observation System (GLOSS), regulations and manuals for sea-level observation and interpretation, and the Permanent Service for Mean Sea Level (PSMSL) is servicing the monthly Mean Sea Level (MSL) provided by countries around the world based on the International Oceanographic Data Exchange (IODE). We used the monthly MSL for our analysis. The Korea Hydrographic and Oceanographic Agency (KHOA) constructs and operates 51 measuring stations, including 45 tidal stations nearby Korean Peninsula. The measuring station additionally measures temperature, atmospheric pressure, wind direction, water temperature, salinity, flow velocity, wave height, and the provided information may vary by each measuring station. Each station measures and collects each data at 1-minute intervals. Since this raw data contains a lot of noise and errors, the KHOA does not recommend using it for direct research purposes. After minimal refinement and interpolation, it provides the tide data at 1-hour intervals. But the data still is not suitable for use in research because it contains many missing values and defects in the data. Therefore, we used only the monthly MSL provided by PSMSL.

References

1. Chen, J., Wilson, C. & Tapley, B. Contribution of ice sheet and mountain glacier melt to recent sea level rise. *Nat. Geosci.* **6**, 549–552 (2013).
2. Church, J. A. *et al.* Revisiting the earth's sea-level and energy budgets from 1961 to 2008. *Geophys. Res. Lett.* **38** (2011).
3. DeConto, R. M. & Pollard, D. Contribution of antarctica to past and future sea-level rise. *Nature* **531**, 591–597 (2016).
4. Rignot, E. *et al.* Four decades of antarctic ice sheet mass balance from 1979–2017. *Proc. Natl. Acad. Sci.* **116**, 1095–1103 (2019).
5. Horton, B. P. *et al.* Estimating global mean sea-level rise and its uncertainties by 2100 and 2300 from an expert survey. *npj Clim. Atmospheric Sci.* **3**, 1–8 (2020).
6. Shepherd, A. *et al.* Mass balance of the antarctic ice sheet from 1992 to 2017. *Nature* **558**, 219–222 (2018).

7. Smith, B. *et al.* Pervasive ice sheet mass loss reflects competing ocean and atmosphere processes. *Science* **368**, 1239–1242 (2020).

8. Robinson, C., Dilkina, B. & Moreno-Cruz, J. Modeling migration patterns in the usa under sea level rise. *Plos one* **15**, e0227436 (2020).

9. Tebaldi, C., Strauss, B. H. & Zervas, C. E. Modelling sea level rise impacts on storm surges along us coasts. *Environ. Res. Lett.* **7**, 014032 (2012).

10. Barnard, P. L. *et al.* Development of the coastal storm modeling system (cosmos) for predicting the impact of storms on high-energy, active-margin coasts. *Nat. hazards* **74**, 1095–1125 (2014).

11. Kriebel, D. L., Geiman, J. D. & Henderson, G. R. Future flood frequency under sea-level rise scenarios. *J. Coast. Res.* **31**, 1078–1083 (2015).

12. Vitousek, S. *et al.* Doubling of coastal flooding frequency within decades due to sea-level rise. *Sci. reports* **7**, 1–9 (2017).

13. Vousdoukas, M. I. *et al.* Global probabilistic projections of extreme sea levels show intensification of coastal flood hazard. *Nat. communications* **9**, 1–12 (2018).

14. Kulp, S. A. & Strauss, B. H. New elevation data triple estimates of global vulnerability to sea-level rise and coastal flooding. *Nat. communications* **10**, 1–12 (2019).

15. Taherkhani, M. *et al.* Sea-level rise exponentially increases coastal flood frequency. *Sci. reports* **10**, 1–17 (2020).

16. Zwally, H. J. *et al.* Mass gains of the antarctic ice sheet exceed losses. *J. Glaciol.* **61**, 1019–1036 (2015).

17. Project, J. M. M. Ghrsst level 4 mur global foundation sea surface temperature analysis (2015). Dataset accessed [2020-08-21] at https://doi.org/10.5067/GHGMR-4FJ04.

18. Hamlington, B. & Thompson, P. Considerations for estimating the 20th century trend in global mean sea level. *Geophys. Res. Lett.* **42**, 4102–4109 (2015).

19. Cazenave, A., Cabanes, C., Dominh, K. & Mangiarotti, S. Recent sea level change in the mediterranean sea revealed by topex/poseidon satellite altimetry. *Geophys. research letters* **28**, 1607–1610 (2001).

20. Cabanes, C., Cazenave, A. & Le Provost, C. Sea level rise during past 40 years determined from satellite and in situ observations. *Science* **294**, 840–842 (2001).

21. Nerem, R. S., Chambers, D. P., Choe, C. & Mitchum, G. T. Estimating mean sea level change from the topex and jason altimeter missions. *Mar. Geod.* **33**, 435–446 (2010).

22. Watson, C. S. *et al.* Unabated global mean sea-level rise over the satellite altimeter era. *Nat. Clim. Chang.* **5**, 565–568 (2015).

23. Kim, Y. & Cho, K. Sea level rise around korea: Analysis of tide gauge station data with the ensemble empirical mode decomposition method. *J. hydro-environment research* **11**, 138–145 (2016).

24. Kim, K.-Y. & Kim, Y. A comparison of sea level projections based on the observed and reconstructed sea level data around the korean peninsula. *Clim. change* **142**, 23–36 (2017).

25. Nerem, R. S. *et al.* Climate-change–driven accelerated sea-level rise detected in the altimeter era. *Proc. Natl. Acad. Sci.* **115**, 2022–2025 (2018).

26. Wöppelmann, G., Miguez, B. M., Bouin, M.-N. & Altamimi, Z. Geocentric sea-level trend estimates from gps analyses at relevant tide gauges world-wide. *Glob. Planet. Chang.* **57**, 396–406 (2007).

27. Houston, J. R. & Dean, R. G. Sea-level acceleration based on us tide gauges and extensions of previous global-gauge analyses. *J. Coast. Res.* **27**, 409–417 (2011).

28. Talke, S., Kemp, A. & Woodruff, J. Relative sea level, tides, and extreme water levels in boston harbor from 1825 to 2018. *J. Geophys. Res. Ocean.* **123**, 3895–3914 (2018).

29. Boretti, A. The pattern of sea-level rise across the north atlantic from long-term-trend tide gauges. *Ocean. & Coast. Manag.* **196**, 105309 (2020).

30. The national atlas of korea. http://nationalatlas.ngii.go.kr/pages/page_1274.php. Accessed: 2021-08-07.

31. Collins, M. *et al.* The impact of global warming on the tropical pacific ocean and el niño. *Nat. Geosci.* **3**, 391–397 (2010).

32. Philander, S. G. H. El nino southern oscillation phenomena. *Nature* **302**, 295–301 (1983).

33. Ropelewski, C. F. & Halpert, M. S. North american precipitation and temperature patterns associated with the el niño/southern oscillation (enso). *Mon. Weather. Rev.* **114**, 2352–2362 (1986).

34. Kumar, K. K., Rajagopalan, B. & Cane, M. A. On the weakening relationship between the indian monsoon and enso. *Science* **284**, 2156–2159 (1999).

35. Santoso, A., Mcphaden, M. J. & Cai, W. The defining characteristics of enso extremes and the strong 2015/2016 el niño. *Rev. Geophys.* **55**, 1079–1129 (2017).

36. Lin, J. & Qian, T. A new picture of the global impacts of el nino-southern oscillation. *Sci. reports* **9**, 1–7 (2019).

37. Huang, N. E. *et al.* The empirical mode decomposition and the hilbert spectrum for nonlinear and non-stationary time series analysis. *Proc. Royal Soc. London. Ser. A: mathematical, physical engineering sciences* **454**, 903–995 (1998).

38. Wu, Z. & Huang, N. E. Ensemble empirical mode decomposition: a noise-assisted data analysis method. *Adv. adaptive data analysis* **1**, 1–41 (2009).

39. Yeh, J.-R., Shieh, J.-S. & Huang, N. E. Complementary ensemble empirical mode decomposition: A novel noise enhanced data analysis method. *Adv. adaptive data analysis* **2**, 135–156 (2010).

40. Torres, M. E., Colominas, M. A., Schlotthauer, G. & Flandrin, P. A complete ensemble empirical mode decomposition with adaptive noise. In *2011 IEEE international conference on acoustics, speech and signal processing (ICASSP)*, 4144–4147 (IEEE, 2011).

41. Colominas, M. A., Schlotthauer, G. & Torres, M. E. Improved complete ensemble emd: A suitable tool for biomedical signal processing. *Biomed. Signal Process. Control.* **14**, 19–29 (2014).

List of Figures

Acknowledgements

This work was supported by National Institute for Mathematical Sciences (NIMS) grant funded by the Korea government (MSIT) (B21710000)

Author contributions statement

Y. J. Kim, O. Kwon, and H. Kang conceived the study. Y. J. Kim conducted pre-processing and managing of all data. Y. J. Kim wrote the manuscript. All authors analyzed the results. All authors reviewed the manuscript.

Additional information

The authors declare no competing interests.

Supplementary Files

This is a list of supplementary files associated with this preprint. Click to download.

- SupplementarymaterialSLRestimationusingCEEMDANneartheKoreanPeninsulaver20211026.pdf